Performance, Emission and Combustion Characteristics of Biodiesel (Waste Cooking Oil Methyl Ester) Fueled IDI Diesel Engine

Article *in* SAE Technical Papers · April 2008

DOI: 10.4271/2008-01-1384

CITATIONS
42

READS
267

2 authors, including:

Avinash Kumar Agarwal
Indian Institute of Technology Kanpur
580 PUBLICATIONS **23,060** CITATIONS

SEE PROFILE

SAE TECHNICAL PAPER SERIES

2008-01-1384

Performance, Emission and Combustion Characteristics of Biodiesel (Waste Cooking Oil Methyl Ester) Fueled IDI Diesel Engine

Bhaskar Mazumdar
Motilal Nehru National Institute of Technology, Allahabad, India

Avinash Kumar Agarwal
Indian Institute of Technology Kanpur, India

Reprinted From: CI Engine Performance for use with Alternative Fuels, 2008 (SP-2176)

ISBN 978-0-7680-1639-0

**2008 World Congress
Detroit, Michigan
April 14-17, 2008**

SAE International™

400 Commonwealth Drive, Warrendale, PA 15096-0001 U.S.A. Tel: (724) 776-4841 Fax: (724) 776-0790 Web: www.sae.org

ISSN 0148-7191

Printed in USA

2008-01-1384

Performance, Emission and Combustion Characteristics of Biodiesel (Waste Cooking Oil Methyl Ester) Fueled IDI Diesel Engine

Bhaskar Mazumdar
Motilal Nehru National Institute of Technology, Allahabad, India

Avinash Kumar Agarwal*
Indian Institute of Technology Kanpur, India

ABSTRACT

Biodiesel (fatty acid methyl ester) is a non-toxic and biodegradable alternative fuel that is obtained from renewable sources. A major hurdle in the commercialization of biodiesel from virgin oil, in comparison to petroleum-based diesel, is its cost of production, primarily the raw material cost. Used cooking oils or waste cooking oils are economical sources for biodiesel production, which can help in commercialization of biodiesel. However, the products formed during cooking/ frying (such as free fatty acids and various polymerized triglycerides) affect the transesterification reaction and the biodiesel properties.

In present experimental investigations, waste-cooking oil obtained from restaurant was used to produce biodiesel through transesterification process and the chemical kinetics of biodiesel production was studied. Biodiesel was blended with petroleum diesel in different proportions. The blends were evaluated for the engine performance, emissions and combustion characteristics in a four-stroke, four-cylinder, indirect injection transportation engine vis-à-vis baseline data of petroleum diesel.

It is observed that mass emission of various regulated pollutant species from biodiesel blends is not significantly different from baseline petroleum diesel. Oxides of nitrogen (NO_x) emissions increased with increasing concentration of biodiesel in blends, while carbon monoxide (CO) emissions decreased. Brake thermal efficiency of biodiesel blends was observed to be higher as compared to petroleum diesel for all blends. Brake specific fuel consumption (bsfc) and Brake specific energy consumption of all biodiesel blends was found to be lower than petroleum diesel and it was found to be lowest for B20. In addition to this, pressure-crank angle diagram for different biodiesel blends at different engine loads were obtained. Detailed combustion analysis such as rate of heat release, cumulative heat release, rate of pressure rise etc. was done for all biodiesel blends vis-à-vis petroleum diesel and the results are discussed in details.

INTRODUCTION

Today the world is confronted with twin crises of fossil fuel depletion and environmental degradation. Indiscriminate extraction and lavish consumption of fossil fuels has led to reduction of underground carbon based resources [1]. Exploring new energy resources such as biodiesel from various edible and non-edible oils such as soyabean, sunflower, jatropha (*Jatropha Curcas*) and karanja (*Pongamia Pinnata*) has been of growing importance in recent years. When Rudolf Diesel invented the diesel engine, he demonstrated it at the 1900 world exhibition in Paris, employing peanut oil as fuel and said “The use of vegetable oils for engine fuels may seem insignificant today, but such oils may become in course of time as important as petroleum and the coal tar products of the present time” [2]. Since then many researchers have investigated this energy resource and concluded that vegetable oils and their derivatives hold promise as alternative fuels for diesel engines rather than spark-ignited engines due to their low volatility and high cetane number. However the increased viscosity and low volatility of vegetable oils lead to severe engine deposits, injector coking, and piston ring sticking [3]. These undesirable effects can be reduced or eliminated through transesterification of the vegetable oil to produce alkyl esters (biodiesel). The process of transesterification removes glycerin from the triglyceride molecules present in vegetable oils and replace it with the alcohol used in the conversion

*Corresponding Author’s email: akag@iitk.ac.in

process. This process decreases the viscosity but maintains the cetane number and the heating value [3]. This conventional biodiesel technology involves use of either a base or acid catalyst at/ near boiling point temperature of triglyceride/ alcohol mixture. The chemical reaction of transesterification is given below.

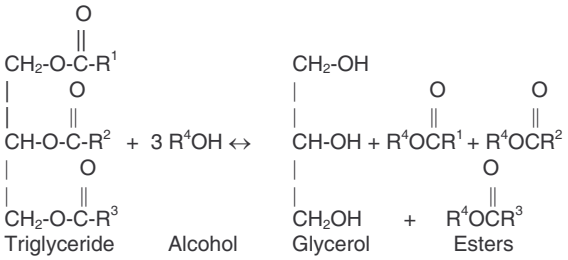

Figure 1: Transesterification reaction

The product formed is vegetable oil methyl ester or biodiesel. In a stoichiometric reaction, three moles of alcohol are required for transesterification of one mole of triglycerides however this is a reversible reaction therefore excess alcohol is required to shift the equilibrium to product side. Conversion rate for base catalyzed transesterification is found to be higher than acid catalyzed transesterification [4, 5, 6] therefore this is the process chosen for the present investigations. Biodiesel is a non-poisonous, biodegradable, and oxygenated fuel, therefore its combustion efficiency in the engine is higher than petroleum diesel. Biodiesel also has inherent lubricity properties [7].

The carbon cycle time for fixation of CO_2 is very small for biodiesel (few years) as compared to petroleum diesel (few million years). Therefore using biodiesel as engine fuel reduces greenhouse gas emissions also [8,9].

A number of engine studies have amply demonstrated that vegetable oils, such as soyabean, safflower, rapeseed, and their esters, are viable alternative fuels for diesel engines. Many researchers have found that diesel engines can run with biodiesel successfully for long durations and the performance and emission characteristics of the unmodified engines is quite comparable to petroleum diesel fueled engines [10-12]. Zhang *et al*. investigated blends of methyl, isopropyl and winterized esters of soybean oil and got significant emission reduction in CO, HC, particulate and solid carbon with identical engine performance [13]. Kalligeros *et al.* conducted test with biodiesel produced from sunflower oil and olive oil in a single cylinder stationary diesel engine and found lower particulate matter, carbon monoxide, hydrocarbons and nitrogen oxide emissions with a slight increase in volumetric fuel consumption [14]. Raheman *et al.* executed performance and emission test on a single cylinder stationary engine and found that CO, smoke, HC and NO_x decreased with the karanja oil methyl ester [15]. Altiparmak *et al.* conducted test with tall oil methyl ester in direct injection diesel engine and found lower CO emissions, lower sulfur content, higher torque and engine power output at higher engine speeds [16]. Ozgunay *et al.* investigated the performance and emission results of biodiesel obtained from leather industry pre-fleshings and found that performance results were quite similar to petroleum diesel with a considerable reduction in particulate and CO emissions [17].

However compared to petroleum-based diesel, higher cost of biodiesel has been a major hurdle in its commercialization. Therefore, waste cooking oil, which is lower cost than raw/ virgin vegetable oil, is a promising alternative for biodiesel production. The quantity of waste cooking oil generated per year by any country is of the order of magnitude of millions of tons. The disposal of waste cooking oil is problematic because disposal methods contaminate ground water and other water bodies. Many developed countries have set forth policies that penalize the disposal of waste oil routed through water drainage. The production of biodiesel from waste cooking oil is one of the better ways to utilize it efficiently and economically thus eliminating the disposal related problems at the same time [18].

The data on the requirements of petroleum diesel and availability of waste cooking oil in any country indicate clearly that biodiesel obtained from waste cooking oils may not replace petroleum diesel completely. However, a substantial amount of diesel fuel can be prepared from waste cooking oil, which would partially decrease the dependency on petroleum-based diesel [18].

BIODIESEL PREPARATION & CHARACTERIZATION

The Biodiesel fuel used in this study was produced from the transesterification of waste cooking oil with methanol (CH_3OH) in presence of sodium hydroxide (NaOH) catalyst. For process optimization, catalyst concentration was kept constant (0.5% w/w_{oil}) and methanol to oil molar ratio was varied from 4.5:1 to 15:1. The reaction time and temperature were kept constant at 1 hour and 60^0C respectively. The yield of biodiesel with the molar ratio of alcohol to oil is shown in figure 2, which shows that maximum biodiesel yield of 98% is obtained for a 9:1 molar ratio of alcohol to oil.

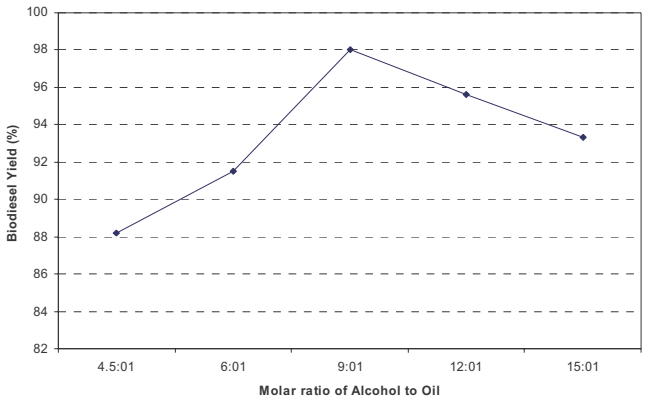

Figure 2: Biodiesel yield (%) for various molar ratios of alcohol to oil

For transesterification of waste cooking oil in laboratory, oil was heated in a round bottom flask upto 60º C. NaOH was dissolved in measured quantity of methanol in a separate flask and was then poured in to round bottom flask, while stirring the mixture continuously. The mixture was maintained at 60°C for one hour. The reaction products were poured into a separating funnel and kept for approx. 6 hours for gravity separation of glycerol with waste cooking oil methyl esters. The glycerol forms lower layer due to higher density, which is separated out. The esters were then washed with (10% v/v) warm water (at 50°C) and kept for about 4 hours in separating funnel to remove the catalyst and excess alcohol present in biodiesel. After removal of water, which forms the lower layer, biodiesel is dried using silica gel and thus the final product is produced. This biodiesel is then blended with petroleum diesel and various blends such as B05, B10, B20, B50, and B100 are prepared for conducting CI engine experiment. Characterization of biodiesel blends and petroleum diesel was also done in laboratory as per the relevant ASTM norms (table 1). Specific gravity of blends was measured using density meter (Make: Kyoto Electronics, Japan, Model: DA-130N). Kinematic viscosity was measured (ASTM D 445) using kinematic viscometer (Make: Stanhope Seta, UK, Model: 83541-3).

Table 1: Fuel Properties

Fuel	Specific Gravity @ 25 C ASTM D 1298	Viscosity @ 40ºC (cSt) ASTM D 445	Cetane Index[19] ASTM D 976	Calorific Value[19] (MJ/kg) ASTM D 240
Diesel	0.833	3.18	46.2	44.80
B05	0.8379	-	--	44.63
B10	0.8384	-	--	44.46
B20	0.844	-	--	44.11
B50	0.8596	-	--	43.08
B100	0.887	4.31	44.28	41.37

EXPERIMENTAL SETUP

A transportation IDI diesel engine (Make: Mahindra & Mahindra Ltd, India, model: XD-3P), typically used in utility vehicles was used for conducting engine tests. The specifications of the engine are given in the table 2. The engine was coupled with Eddy current dynamometer (Make: Schenck Avery, India; Model: ASE 50) for simulating test conditions. Data for engine speed (rpm), torque (N-m), inlet and outlet cooling water temperature, exhaust gas temperature etc. was collected from appropriate points using different types of sensors. Engine speed and load were controlled by varying excitation current to the eddy current dynamometer.

Exhaust gas emissions were measured using raw exhaust gas analyzer (Make: Horiba, Japan; Model: EXSA-1500). It measures CO and CO_2 by NDIR detector, Total hydrocarbons (THC) by heated flame ionization detector (hot FID) and NO_x by Chemiluminescence detector. The equipment was installed with heated sample gas piping maintained at 191°C to prevent condensation of moisture present in the exhaust. Exhaust gas opacity was measured using exhaust gas opacimeter (Make: AVL, Austria; Model: 437).

Table 2: Specifications of the engine

Manufacturer	M&M Ltd, India
Model	XD-3P
Type of Engine	Four stroke, water cooled, naturally aspirated pre-chamber design
Number of Cylinders	Four
Bore/ Stroke	94/ 90 (mm)
Displacement volume	2498 cc
Compression ratio	23:1
Rated Power	72.5 hp @ 4000 rpm without Oil Cooler
Max. Torque	125 Nm @ 2000 rpm

Cylinder pressure was measured using piezoelectric pressure transducer (Make: AVL, Austria; Model: GU21C), which was installed in the engine cylinder head. The pressure transducer was mounted flush with the auxiliary chamber in the head of cylinder 1 so that the distortions due to torsion of crankshaft is minimized.

A high precision inductive shaft encoder (Model AVL 333; Make: AVL Austria) was used for detecting crank angle rotation with a precision of 0.1 crank angle degrees (CAD). A magnetic pickup was used sending the TDC. It was mounted on a frame connected to the base of the engine. A twin channel high speed data acquisition system (Make: AVL, Austria; Model: Indimeter-619) was used for recording and analyzing the pressure crank angle data.

The schematic layout of the experimental setup is shown in figure 3.

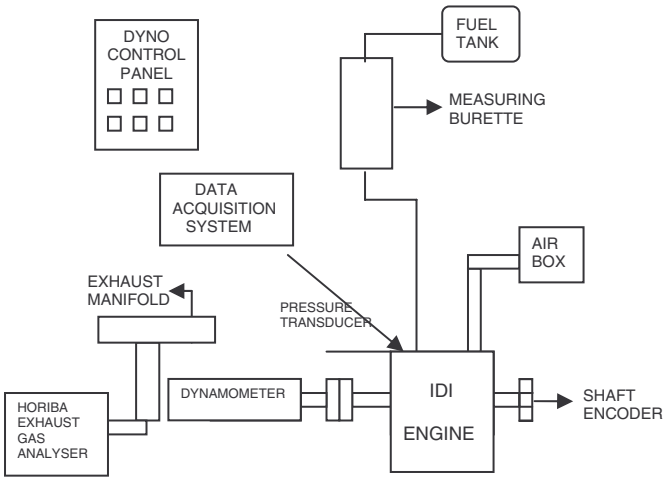

Figure 3: Schematic Diagram of the Experimental Setup

Engine tests were conducted according to Indian Standard Codes [20-22]. According to this, engine performance parameters such as power output, efficiency, emissions, smoke opacity etc. were measured for each fuel blend. The engine was operated at a constant speed of 2000 rpm (rated speed for maximum torque) and data collection for performance, emission and combustion parameters was done. The data were recorded at various loads of 0, 25, 50, 75,100 and 125 Nm. Before recording the data, sufficient time was allowed for the engine to stabilize and then three readings were taken. The average of the three readings was analyzed and reported in this paper.

RESULTS AND DISCUSSION

The data were collected and analyzed under three sub-headings. The results are presented for performance parameters, emission parameters and combustion parameters.

PERFORMANCE RESULTS

The engine performance is analyzed in the form of thermal efficiency, bsfc, bsec and exhaust gas temperature.

The brake thermal efficiency of different biodiesel blends vis-à-vis petroleum diesel is shown in figure 4a.

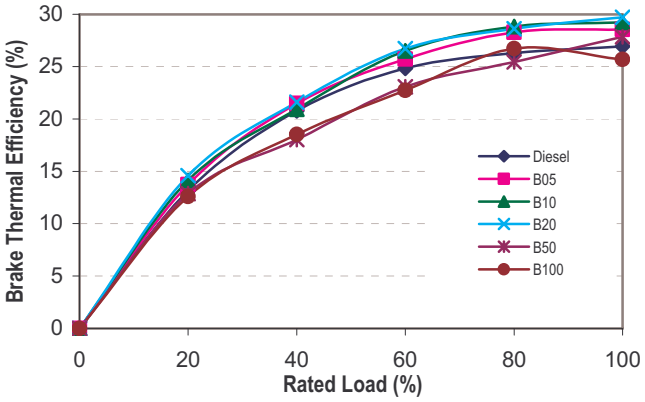

Figure 4a: Brake thermal efficiency of different biodiesel blends

From the figure 4a, it is evident that brake thermal efficiency of all biodiesel blends is higher than petroleum diesel. Biodiesel blends have generally higher thermal efficiency inspite of their relatively lower heating value. It is observed that B20 has highest thermal efficiency among all biodiesel blends.

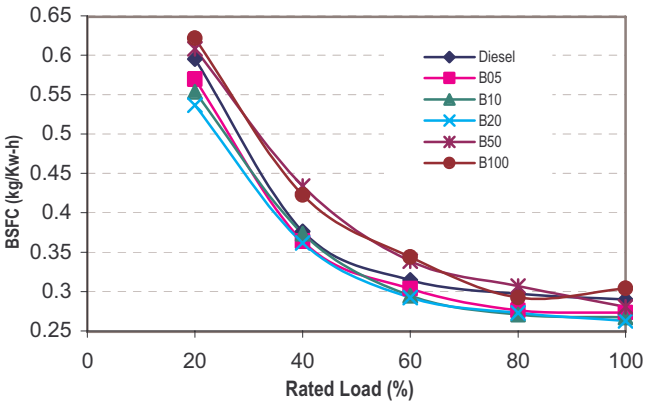

Figure 4b: BSFC for different biodiesel blends

For brake specific fuel consumption (bsfc), higher biodiesel blends show slightly higher bsfc than petroleum diesel, because the heating value of the biodiesel is lower than petroleum diesel. B20 however demonstrates lowest bsfc. Brake specific fuel consumption is however not a scientifically rationale parameter to compare the performance of fuels having different calorific values. Brake specific energy consumption is a more relevant parameter to compare the engine performance in such a situation. Figure 4c represents bsec for different biodiesel blends.

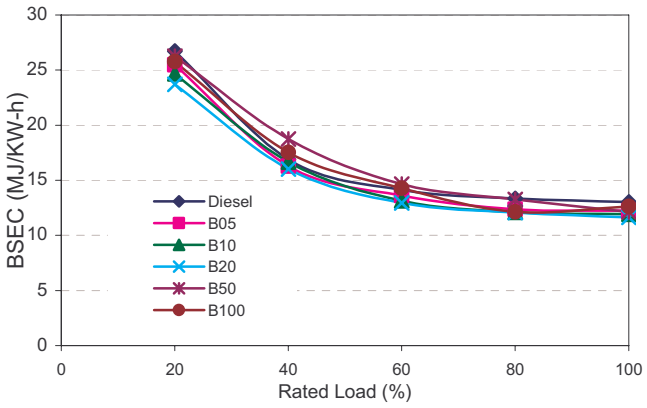

Figure 4c: BSEC for different biodiesel blends

The lower Biodiesel blends (upto B20) show lower bsec as compared to petroleum diesel for all the loads, proving that the lower blends are more efficient, in terms of energy consumption. However the higher blends (B50 and B100) have almost similar bsec as that of petroleum diesel. It can be observed that B20 has lowest bsec under all operating conditions. In addition to this, with increasing engine load, a decreasing trend of brake specific energy consumption (bsec) has been observed.

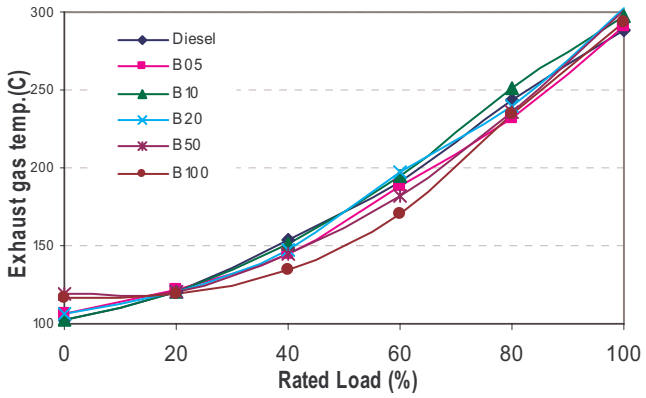

Figure 4d: Exhaust gas temperature for different biodiesel blends

The exhaust gas temperatures for different fuels are shown in figure 4d. The exhaust gas temperatures for all biodiesel blends and petroleum diesel were in a narrow band. Exhaust gas temperatures were generally slightly higher for biodiesel blends compared to petroleum diesel and this difference decreases at higher engine loads.

EMISSION CHARACTERISTICS

The biodiesel fueled engine emits several regulated and unregulated pollutant species. This study is limited to observe the regulated pollutants. The emissions were recorded using the raw exhaust gas emission analyzer. These emission were then converted to mass emissions using the SAE standard and Indian Standard [22].

HC emission: it is observed from figure 5a that all biodiesel blends have lower HC emissions as compared to petroleum diesel at lower engine loads. With increasing blend concentration, HC emissions decrease. This is because biodiesel is an oxygenated fuel having 10- 11% oxygen content by weight [23].

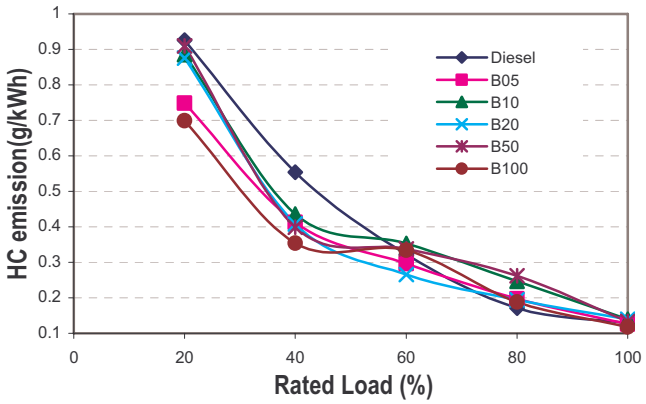

Figure 5a: Total hydrocarbon (THC) mass emissions for different biodiesel blends

With increasing amount of biodiesel in blends, the amount of oxygen in the fuel increases, which support more complete combustion hence lesser particulate and hydrocarbon emissions. B100 shows lowest emissions for most of the engine operating conditions. Also, a general trend is that with increasing engine load, HC mass emissions decrease, which is due to increasing pressure and temperature in the combustion chamber which in turn improves the combustion of the fuel. At higher loads, some blends show comparable emissions with petroleum diesel however these absolute values are negligible.

CO emission: From figure 5b, it is clear that upto 60% engine load (75 Nm), all biodiesel blends show significantly lower CO mass emissions compared to petroleum diesel. This is due to presence of fuel oxygen in biodiesel. Again B100 shows lowest CO emission for all engine operating conditions. At higher loads B05, B10, B20 and B50 have almost similar CO mass emission as petroleum diesel however the values are really insignificant.

With increasing engine load, CO emission increases due to lower availability of oxygen (due to reduction in overall air/ fuel ratio). However the higher fuel injected also produces higher amount of useful work thus lowering the overall reduction in mass emission of carbon monoxide [22]. As a result the trend is looks reverse.

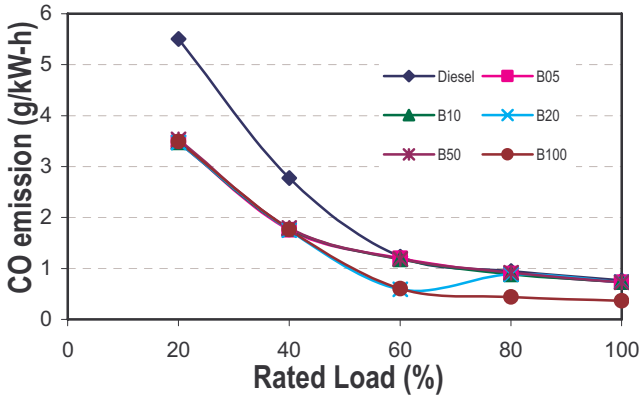

Figure 5b: Carbon monoxide (CO) mass emissions for different biodiesel blends

NO_x emission: The trend of NO_x emission can be seen in figure 5c. NOx emissions depend upon the temperature of the combustion chamber and oxygen availability in the combustion chamber. NOx has fuel as well as thermal origin.

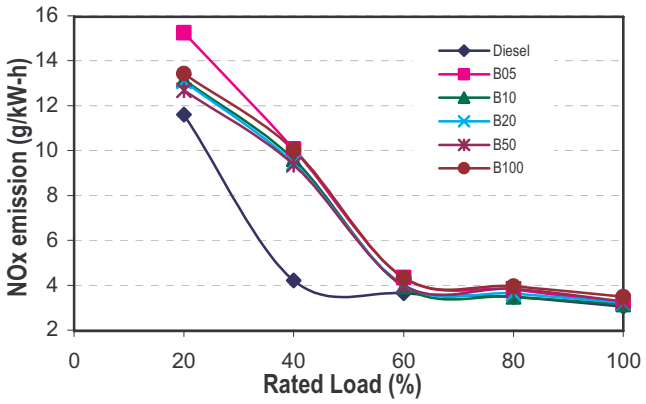

Figure 5c: NO_x mass emissions for different biodiesel blends

By observing the experimental data, it can be noticed that the 40% NOx emission data for the mineral diesel seem to be an outlier point. After ignoring this data point, it can be seen all biodiesel blends show alightly higher NO_x emissions compared to petroleum diesel at all loads. This can be attributed to the fact that NO_x emissions depend upon temperature of the combustion chamber. Since biodiesel is an oxygenated fuel, therefore it supports more complete combustion of the fuel as a result the temperature of the combustion chamber also gets elevated to higher level, resulting in relatively higher NO_x formation. There is higher fuel oxygen, which also increases the fuel NO_x formation. Also, an overall increase in volumetric raw NO_x emission can be observed with increase in engine load due to increase in temperature of combustion chamber. However since these are mass emissions [22], the trend looks reverse.

Smoke Opacity: Smoke opacity has a direct relationship with the amount of particulate in the exhaust. If smoke opacity is higher, it suggests that particulate emission is higher and vice versa. Figure 5d shows the smoke opacity of different biodiesel fuels in comparison to petroleum diesel.

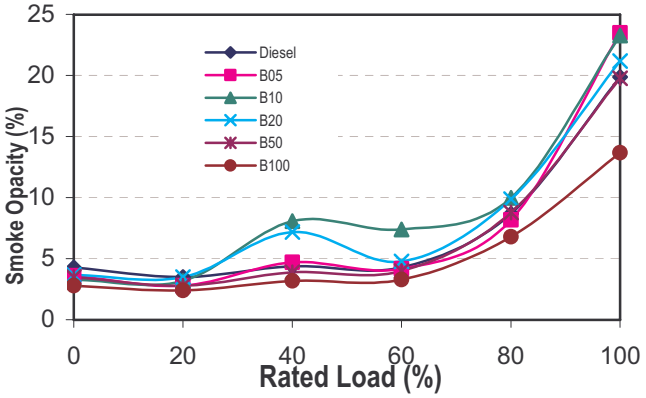

Figure 5d: Smoke opacity for different biodiesel blends

Figure shows that higher biodiesel blends (B50 and B100) show lower smoke opacity at all engine loads compared to petroleum diesel, while lower biodiesel blends (B10 and B20) show relatively higher smoke opacity at higher engine loads (50-125 Nm). Lower smoke opacity of higher blends is due to higher amount of fuel oxygen available, which results in improved combustion and lesser particulate formation. Also, with increasing engine load, smoke opacity increases because of injection of higher amount of fuel, which results in higher number of localized fuel rich regions, which leads to inefficient combustion and thus higher smoke opacity.

COMBUSTION CHARACTERISTICS

A detailed experimental description of combustion evolution in diesel engines is extremely complex because of the simultaneous formation and oxidation of air/fuel mixture. Moreover, knowledge of the combustion process, even in global terms, is extremely useful if we are to better understand the mechanisms governing a greater or lesser concentration of pollutants in the exhaust gas.

A high-speed data acquisition system, a precision shaft encoder and a sensitive piezo-electric pressure transducer was used for acquiring data at a very high speed from the combustion chamber of the IDI engine using various biodiesel blends. This data was then analyzed and presented in the form of pressure-crank angle diagrams, instantaneous heat release diagram, cumulative fuel release diagrams, rate of pressure rise, mass burn fraction diagrams, combustion duration etc.

In-cylinder pressure vs. crank angle diagram

The cylinder pressure data were recorded for fifty consecutive cycles and than averaged out in order to eliminate the effect of cycle to cycle variations. All tests were carried out under steady state engine conditions. The details about combustion stages and events can often be determined by analyzing heat release rates. The trend of heat release (instantaneous heat release rate and cumulative heat release) can be obtained by processing in-cylinder pressure data. The analysis for heat release rate is based on the application of the first law of thermodynamics for an open system. It is assumed that cylinder contents are homogeneous mixture of air and combustion products and are at uniform temperature and pressure at each instant in time during the combustion process.

Here the dotted line shows the motoring curve. The motoring curve displays pressure variation about Top dead centre (TDC) when the engine is working without fuel supply. A symmetrical curve about the top dead centre is expected for better motoring characteristics.

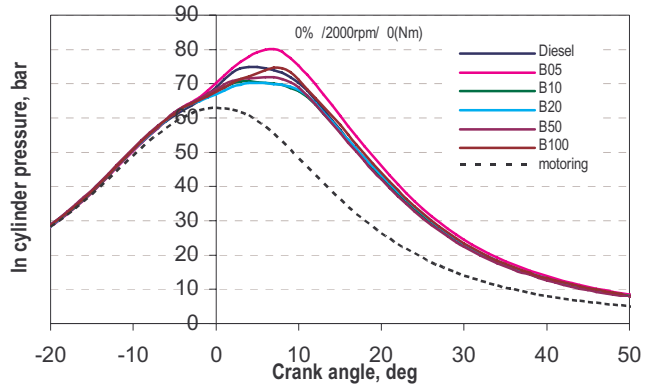

Figure 6a: Pressure crank angle history for different biodiesel blends at no load, 2000 rpm.

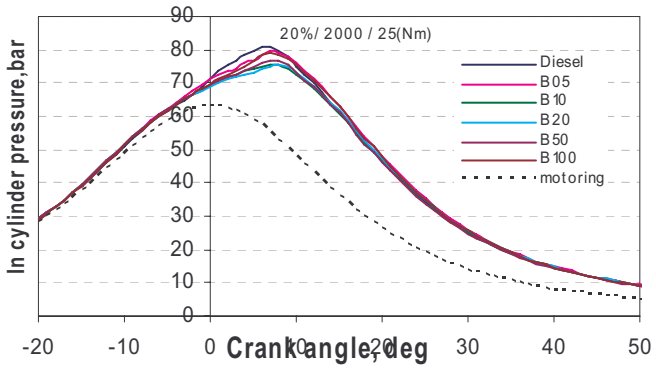

Figure 6b: Pressure crank angle history for different biodiesel blends at 20% load, 2000 rpm.

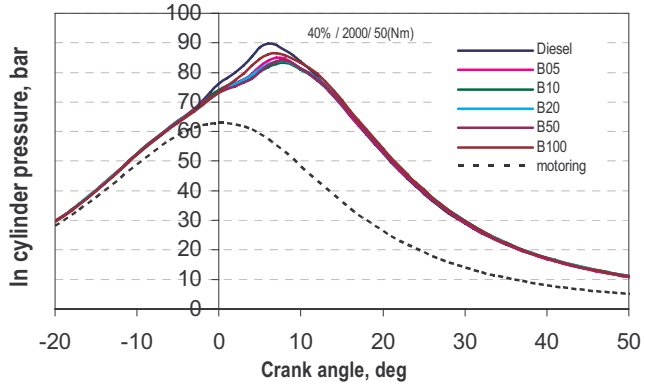

Figure 6c: Pressure crank angle history for different biodiesel blends at 40% load, 2000 rpm.

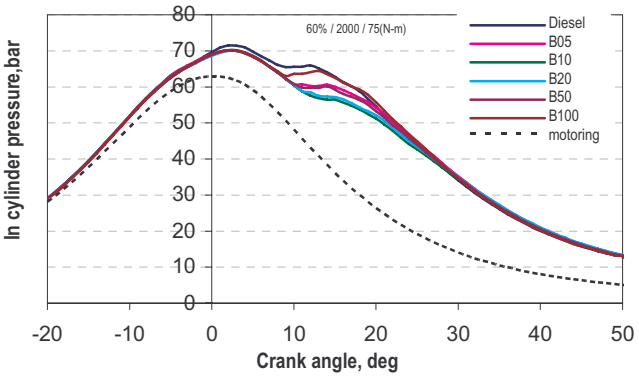

Figure 6d: Pressure crank angle history for different biodiesel blends at 60% load, 2000 rpm.

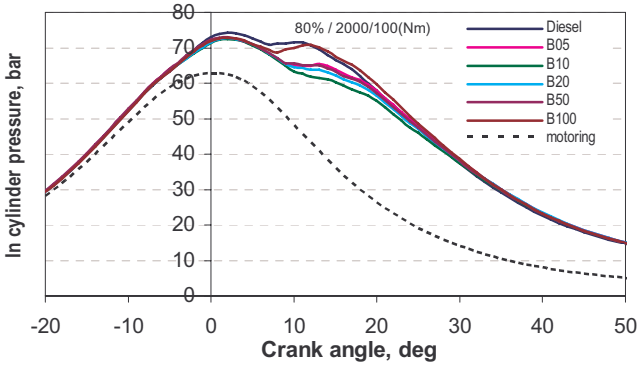

Figure 6e: Pressure crank angle history for different biodiesel blends at 80% load, 2000 rpm.

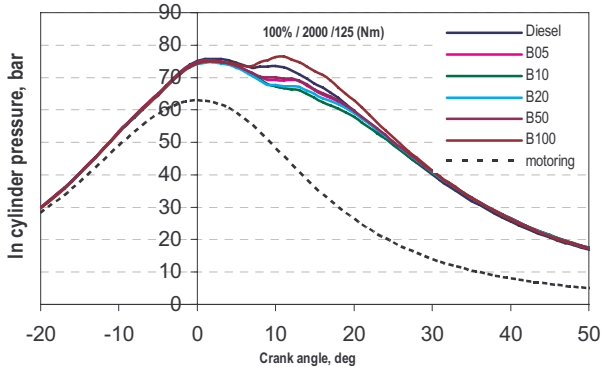

Figure 6f: Pressure crank angle history for different biodiesel blends at 100 % load, 2000 rpm.

Figures 6a-f show the pressure crank angle history for different biodiesel blends at different engine loads. It can be seen that even at lower engine load, the peak cylinder pressure is in the range of 70 to 90 bars. This might be attributed to the possible presence of methanol in biodiesel blends in trace amounts, which vaporizes during premixed combustion phase leading to rise in cylinder pressure. It can also be seen from the figures that a second smaller peak has emerged at higher engine loads (above 50% rated load) because at higher engine loads, higher amount of fuel is injected and some of the fuel burns in late combustion phase, which results in second lower peak. This can be verified from the rate of heat release diagrams also. It can also

be seen from figure 6 that peak pressure emerges at 7-8 crank angle degrees after the top dead center. Also it can be observed that the peak cylinder pressure at idle appears to be much higher than at 100% load , which might be due to the fact that the peak pressure occurs later in the expansion stroke, where the cylinder volume is relatively larger, thus higher amount of energy is liberated in larger cylinder volume, leading to lower peak cylinder pressure.

Instantaneous heat release diagram

Figures 7a-f show the instantaneous heat release diagrams for different biodiesel blends at different engine loads.

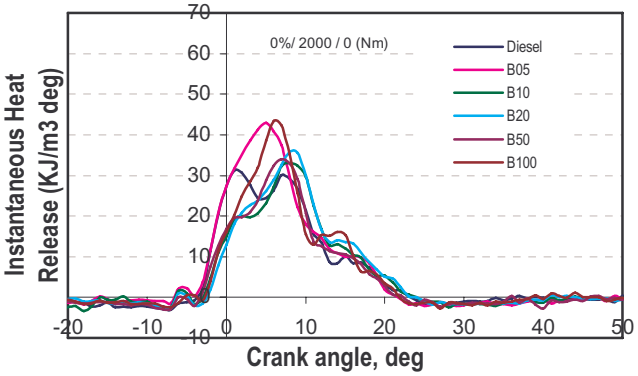

Figure 7a: Instantaneous heat release for different biodiesel blends at no load, 2000 rpm

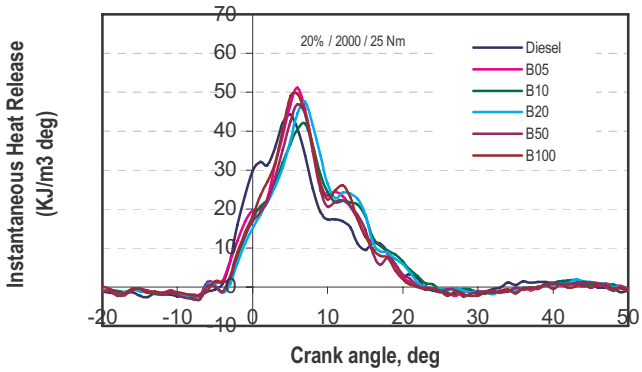

Figure 7b: Instantaneous heat release for different biodiesel blends at 20% load, 2000 rpm

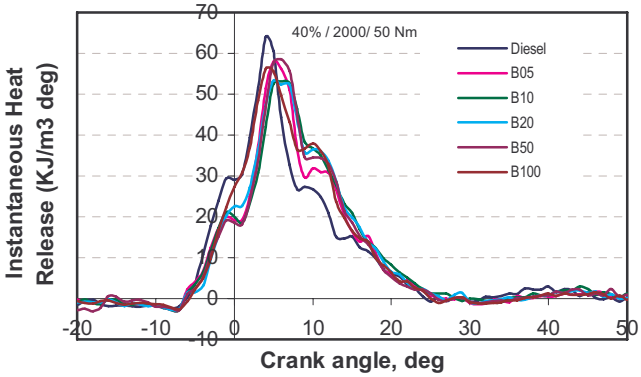

Figure 7c: Instantaneous heat releases for different biodiesel blends at 40% load, 2000 rpm

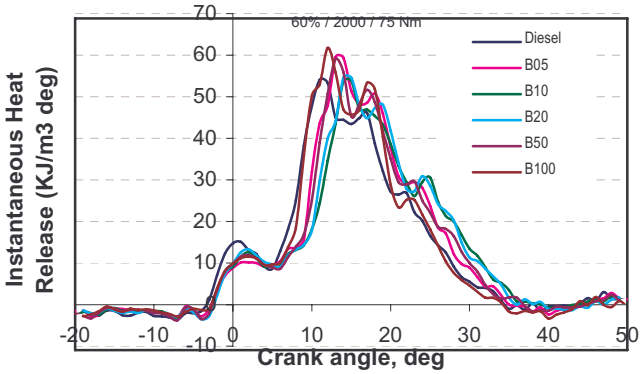

Figure 7d: Instantaneous heat release for different biodiesel blends at 60% load, 2000 rpm

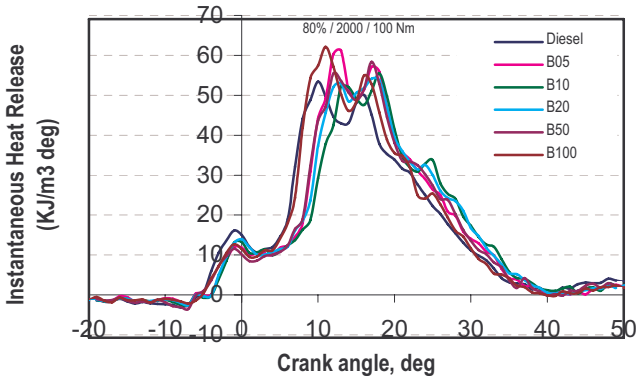

Figure 7e: Instantaneous heat release for different biodiesel blends at 80% load, 2000 rpm

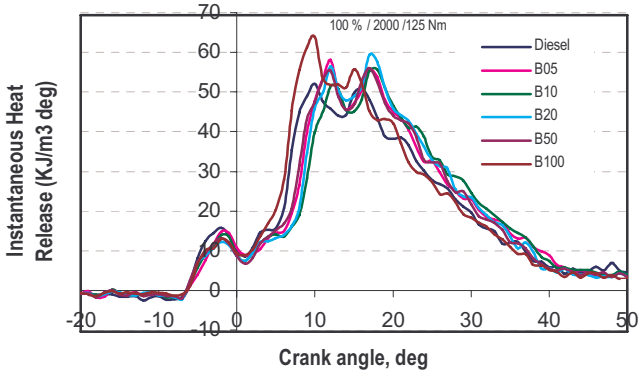

Figure 7f: Instantaneous heat release for different biodiesel blends at 100% load, 2000 rpm

Four phases of combustion, namely ignition delay, premixed combustion phase, mixing controlled combustion and late combustion phases are clearly visible in these diagrams. It can be observed that B05 has shortest ignition delay at lower engine loads, whereas B20 has longest ignition delay at lower loads (figure 7a and 7b). This is also reconfirmed in figure 8(a) and 8(b) for cumulative heat release. Ignition delay is the time required by the fuel to prepare itself for the initiation of combustion. It can be seen from these figures that for lower engine loads, most of the heat release takes place in premixed combustion phase (first peak) and as the lag increases, the mixing controlled combustion phase (second peak) starts dominating. It

can also be seen that petroleum diesel has relatively higher premixed combustion heat release, which is responsible for higher peak pressure at lower engine loads (figure 6). Overall, it can be concluded that heat release diagrams of all biodiesel blends are quite comparable to that of petroleum diesel.

Cumulative heat release diagram

Figure 8 shows cumulative heat release diagrams for various biodiesel blends at different engine loads. It can be noticed from all the figures that there is a negative heat release for all fuels before the top dead center, which is due to absorption of heat required for fuel evaporation and mixing in the combustion chamber.

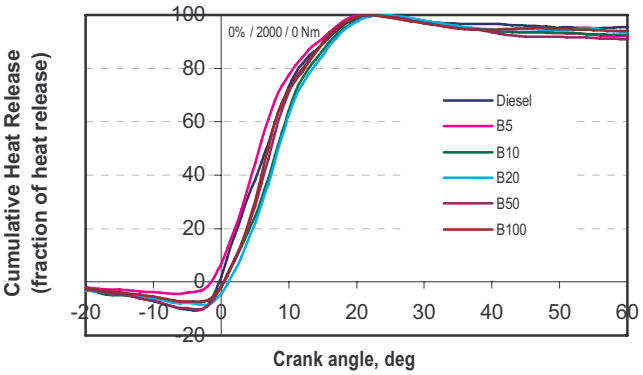

Figure 8a: Cumulative heat release diagram for different biodiesel blends at no load, 2000 rpm

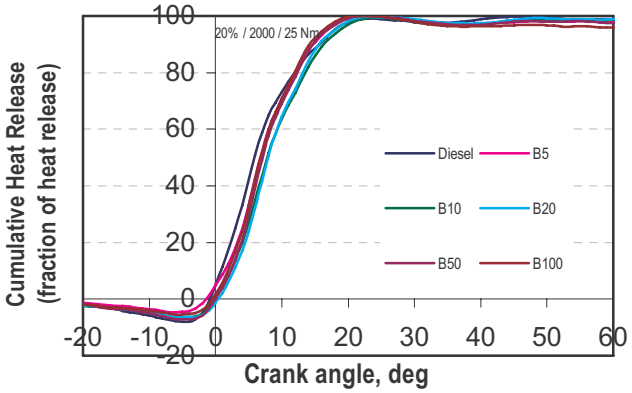

Figure 8b: Cumulative heat release diagram for different biodiesel blends at 20% load, 2000 rpm

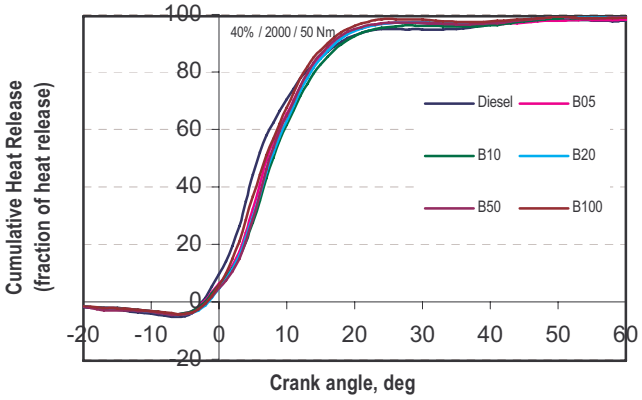

Figure 8c: Cumulative heat release diagram for different biodiesel blends at 40% load, 2000 rpm

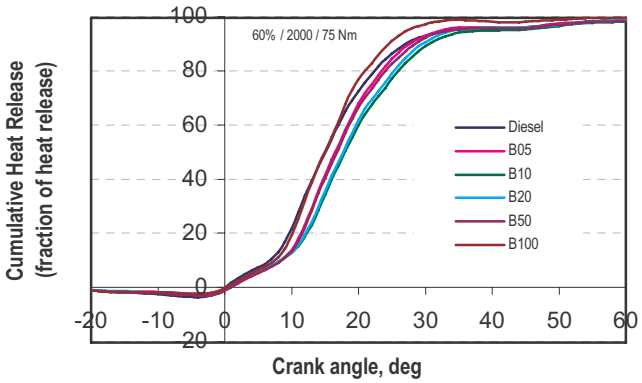

Figure 8d: Cumulative heat release diagram for different biodiesel blends at 60% load, 2000 rpm

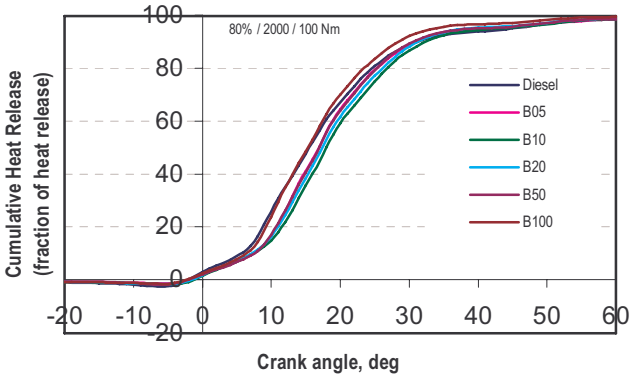

Figure 8e: Cumulative heat release diagram for different biodiesel blends at 80% load, 2000 rpm

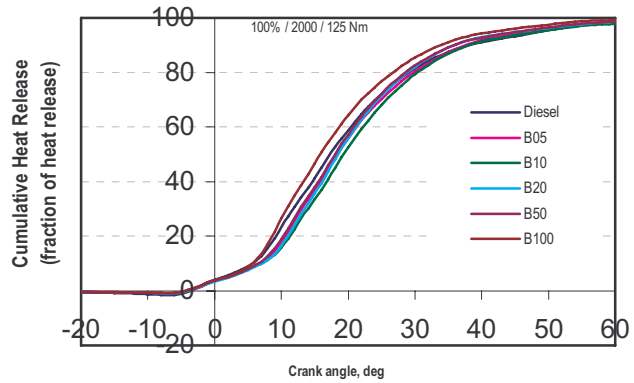

Figure 8f: Cumulative heat release diagram for different biodiesel blend at 100% load, 2000 rpm

It can be seen from the figure 8 that cumulative heat release for B05, B20 & B100 was higher than diesel, which might be due to presence of small amounts of residual methanol in biodiesel, which burns and increases the heat release in the initial/ middle stages of combustion. This can also be due to improved combustion of biodiesel since it has higher cetane number delivering improved combustion characteristics [23]. Also, it can be seen from figures 8 that heat release starts 3-4º before top dead center (bTDC) because combustion starts initially in pre-chamber of the IDI engine and then the burning fuel-air mixture is thrown into the main combustion chamber [23].

Rate of pressure rise diagram

Rate of pressure rise in the main combustion chamber of the engine is an important parameter, which governs the transfer of thrust from combusting gases to the mechanical linkage (power assembly). Rate of pressure rise diagrams for different biodiesel blends are shown in figure 9a-f.

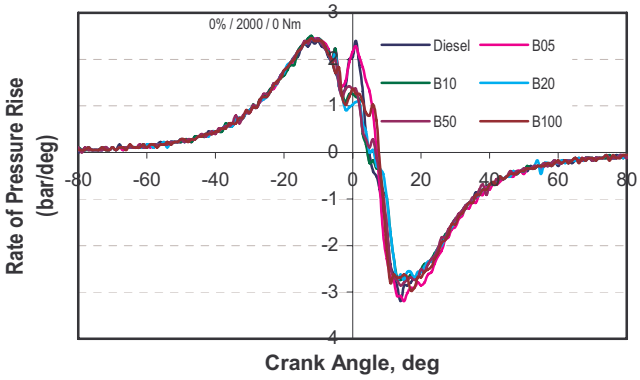

Figure 9a: Rate of pressure rise for different biodiesel blends at no load, 2000 rpm

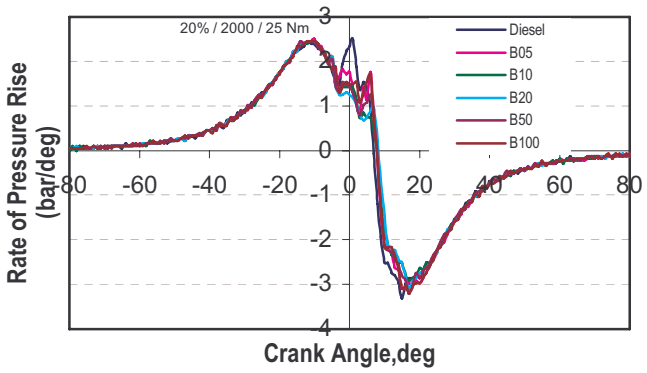

Figure 9b: Rate of pressure rise for different biodiesel blends at 20% load, 2000 rpm

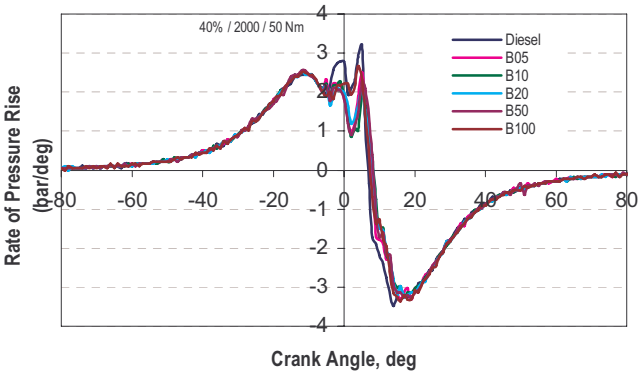

Figure 9c: Rate of pressure rise for different biodiesel blends at 40% load, 2000 rpm

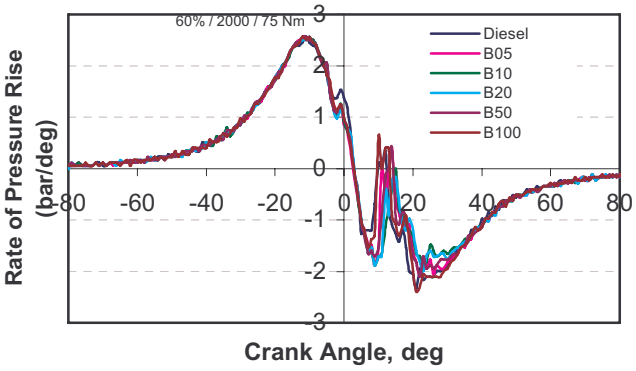

Figure 9d: Rate of pressure rise for different biodiesel blends at 60% load, 2000 rpm

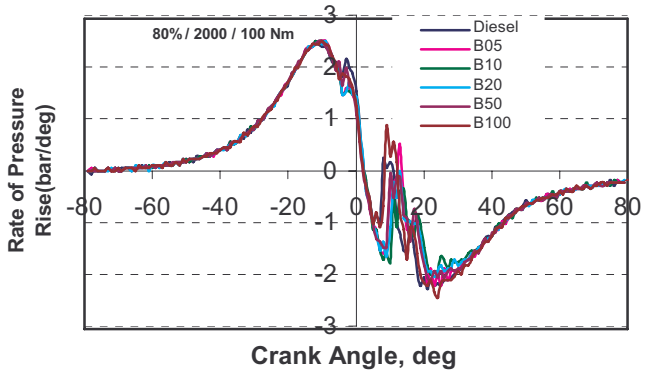

Figure 9e: Rate of pressure rise for different biodiesel blends at 80% load, 2000 rpm

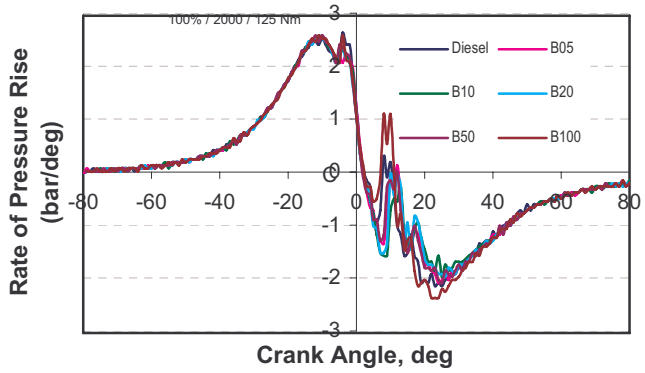

Figure 9f: Rate of pressure rise for different biodiesel blends at 100% load, 2000 rpm

It is observed from the figure 9 that at lower engine loads for all the biodiesel blends and petroleum diesel, a peak is observed which characterizes the start of combustion in pre-chamber after elapse of ignition delay period, which is predominantly premixed combustion phase. This event occurs at 7-8º before top dead center (bTDC). Also, some spikes are seen for some of the blends, which is due to extra heat release at near the TDC, which might be due to presence of traces of methanol. It can also be observed that at higher engine loads, a second peak is observed at 10-12º after top dead center (aTDC) for all the blends. This peak is also seen in the pressure- crank angle diagrams (figure 6). This is due to the fact that more fuel is injected at higher loads. Some of this fuel goes into the main chamber, which burns during late combustion phase, giving rise to second peak. B100 has higher rate of pressure rise in late combustion phase compared to other blends.

Crank angle vs. mass fraction burn diagram

Crank angle duration from 5% mass burn to 90% mass burn has been taken as the combustion duration for comparing the different biodiesel blends.

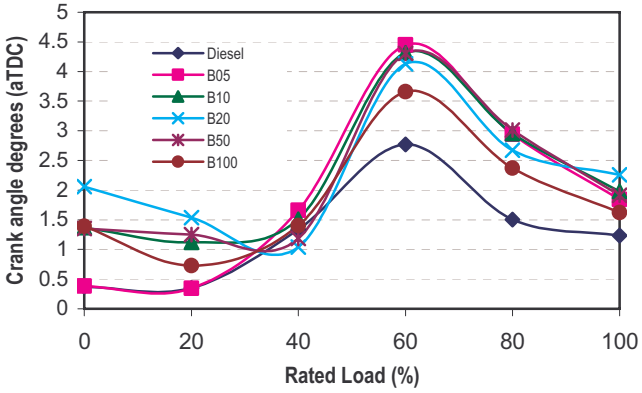

Figure 10a: Crank angle for 5% mass burnt for different biodiesel blends at 2000 rpm

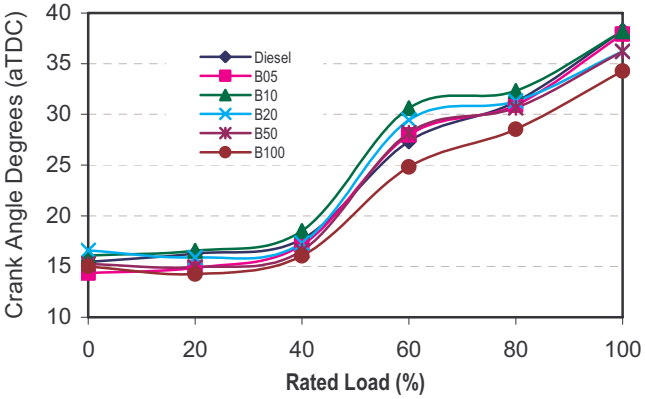

Figure 10b: Crank angle for 90% mass burnt for different biodiesel blends at 2000 rpm

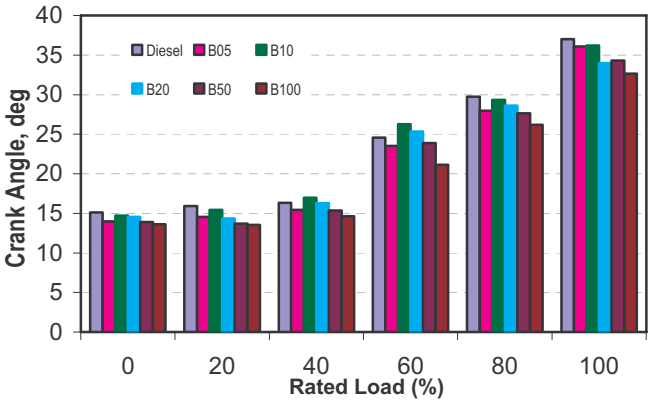

Figure 10c: Variation in combustion duration at 2000rpm

The crank angle degree for 5% mass fraction burned is shown in figure 10a and 90% mass fraction burned is shown in figure 10b. The difference between the two durations is combustion duration, which is shown in the form of a bar chart in figure 10c.

It can be observed from the figure 10a that combustion of B05 starts fastest at about 0.4º aTDC. This is possibly due to its smallest ignition delay. B20 has the maximum delayed start of combustion. From figure 10b and 10c, it is clear that B100 shows fastest 90% mass burn rate, whereas B10 shows slowest mass burn rate. Diesel has highest combustion duration at some loads. It is observed that with increasing

amount of biodiesel in blends, combustion duration decreases, possibly due to advanced injection timing (because of relatively higher bulk modulus of biodiesel) of biodiesel blends and oxygenated nature. In general, combustion duration increases with increasing engine load due to increase in the quantity of fuel injected.

Maximum cylinder pressure, crank angle of peak pressure and maximum rate of pressure rise

It is observed that peak pressure of petroleum diesel is highest under all operating conditions. Maximum cylinder pressure is obtained at 40% rated load (50 Nm) for all biodiesel blends and petroleum diesel. Diesel has 90 bar cylinder pressure at 50 Nm, while B20 is observed to have lowest peak pressure under all operating conditions. Also, at higher engine loads, relatively lower peak cylinder pressures are witnessed in figure 1.

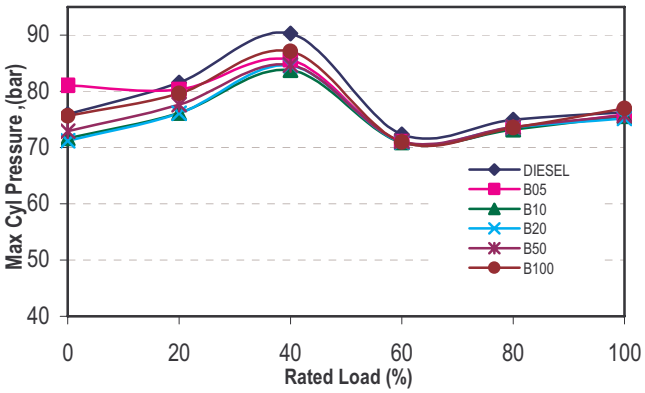

Figure 11: Maximum cylinder pressure for Biodiesel blends at 2000 rpm

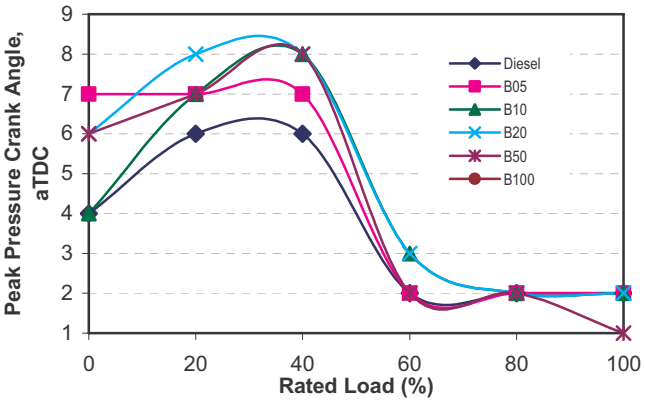

Figure 12: Crank angle for peak pressure for Biodiesel blends at 2000 rpm

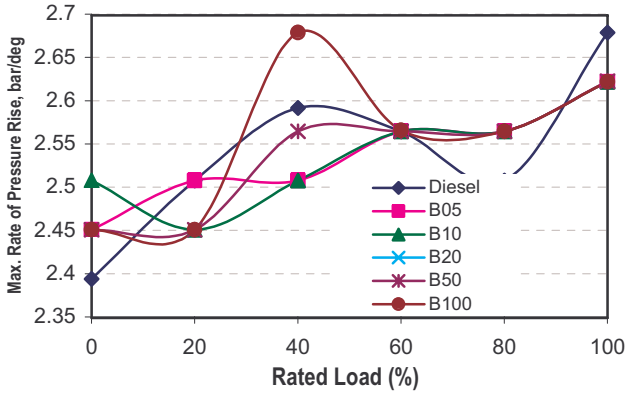

Figure 13: Maximum rate of pressure rise for different biodiesel blends at 2000 rpm

It can be noticed from figure 11 that peak cylinder pressure is attained rather quickly for petroleum diesel under all operating conditions. Also, with increasing engine loads, peak pressure is achieved at lower crank angle degrees (figure 12) possibly due to faster combustion and higher pressure and temperature of main combustion chamber at high engine loads. At 40% rated engine load (50Nm), all biodiesel blends have maximum crank angle (aTDC) for peak pressure. Maximum cylinder pressure depends largely on combustion duration. One can clearly see that at lower loads up to 40%, the combustion duration is of the order of 15 crank angle degrees, therefore the maximum cylinder pressure continuously rises. At loads higher than 40%, the combustion duration also increases up to 35 crank angle degrees (at rated load) and now the heat is released when the cylinder volume is larger leading to reduction in peak cylinder pressure. Maximum rate of pressure rise (figure 13) increases with increasing load except for B100, which has highest maximum rate of pressure rise at 40% rated load.

CONCLUSIONS

In the present investigations, transesterification reaction conditions are optimized for waste cooking oil. The optimum conditions are (9:1 methanol to oil molar ratio at 60°C temperature, NaOH catalyst 0.50% (w/w_{oil}), and 1 hour reaction time. Waste cooking oil methyl ester has a viscosity of 4.32 cSt at 40°C and specific gravity of 0.887, which are very close to that of petroleum diesel. Several blends of biodiesel and petroleum diesel were prepared ranging from 5-50% and the performance, emissions and combustion characteristics of these fuels in transportation IDI CI engine were compared with baseline data generated from petroleum diesel.

Brake thermal efficiency of biodiesel blends was observed to be slightly higher than petroleum diesel for lower blends. Brake specific fuel consumption (bsfc) and brake specific energy consumption (bsec) of lower biodiesel blends (upto B20) was found to be lower than petroleum diesel. In addition to this, exhaust gas temperatures for biodiesel blends was found to be quite comparable to petroleum diesel. Biodiesel

showed slightly lower emissions except NO_x (oxides of nitrogen) emissions and all emissions are well within the acceptable limits.

Combustion characteristics of waste cooking oil biodiesel were also investigated and the results were quite comparable to petroleum diesel. At lower loads, lower blends of biodiesel showed higher peak pressure compared to petroleum diesel. Also, at higher engine loads, a second rise in pressure peak was observed in P-θ curve as well as rate of pressure rise curve, which resembled typical IDI engine characteristics curve. In addition to this, an earlier heat release was observed for lower biodiesel blends before top dead centre (bTDC).

Based on all these detailed performance, emission and combustion investigations, it can be concluded that biodiesel derived from waste cooking oil has the capability to become partial substitute for petroleum diesel in near future and its adoption as a fuel in not expected to lead to any undesirable environmental engine issues.

REFERENCES

1. Agarwal A K, Biofuels (alcohols and biodiesel) applications as fuels for internal combustion engines, Progress in Energy and Combustion Science, 33, 2007, pp 233–271.
2. Krawczyk T, Biodiesel– Alternative fuel makes inroads but hurdle remains, INFORM 7, 1996, pp 801-815.
3. Sinha S, Agarwal A K, Performance evaluation of a biodiesel (rice bran oil methyl ester) fuelled transport diesel engine, SAE 2005-01-1730.
4. Freedman B, Pryde E H, Mounts T L, Variables affecting the yields of fatty esters from transesterified vegetable oils, JAOCS, 61, 1984, pp 1638-1643.
5. Ma F, Hanna M A, Biodiesel production: a review, Bioresource Technology, 70, 1999, pp1-15.
6. Canakci M, VanGerpen G, Biodiesel production via acid catalysis, Transactions of ASAE, 42, 1999, pp 1203-1210.
7. Dorado M P, Ballesteros E, Arnal J M, Gomez J, Lopez F J, Exhaust emissions from a diesel engine fueled with transesterified waste olive oil, Fuel, 82, 2003, pp 1311–1315.
8. Ali Y, Hanna M A, Alternative diesel fuels from vegetable oils, Bioresource Technology, 50, 1994, pp153-165.
9. Senatore A, Cardone M, Rocco V, Prati M V, A Comparative analysis of combustion process in di diesel engine fueled with Biodiesel and diesel fuel, SAE 2000-01-0691.
10 Altin R, Cetinkaya S, Yucesu H S, The potential of using vegetable oil fuels as fuel for diesel engine, Energy conversion & management, 42, 2001, pp 529-538.
11. Scholl K W, Sorenson S C, Combustion of soybean oil methyl ester in a direct injection diesel engine, SAE 930934.
12. Srivastava A, Prasad R, Triglycerides-based diesel fuels, Renewable and Sustainable Energy Reviews, 2000, 4, pp 111-133.
13. Zhang Y, VanGerpen J H, Combustion analysis of esters of soybean oil in a diesel engine, SAE 960765
14. Kalligeros S, Zannikos F, Stournas S, Lois E, Anastopoulos G, Teas C, Sakellaropoulos F, An investigation of using biodiesel/ marine diesel blends on the performance of a stationary diesel engine, Biomass and Bioenergy, 2003, pp 141–149.
15. Raheman H, Phadatare A G, Diesel engine emissions and performance from blends of karanja methyl ester and diesel, Biomass & Bioenergy, 27, 2004, pp 393-397.
16. Altıparmak D, Keskin A, Koca A, Gürü M, Alternative fuel properties of tall oil fatty acid methyl ester–diesel fuel blends, Bioresource Technology, 98, 2007, pp 241–246.
17. Ozgunay H, Colak S, Zengin G, Sari O, Sarikahya H, Yuceer L, Performance and emission study of biodiesel from leather industry pre-fleshings, Waste Management, 27(12), 2007, pp 1897-1901.
18. Kulkarni M G, Dalai A K, Waste cooking oils, an economical source for biodiesel: a review, *Ind. Eng. Chem. Res.* 2006**,** *45, pp* 2901-2913.
19. Lin Y F, Wu Greg Y-P, Chang C T, Combustion characteristics of waste oil produced biodiesel / diesel fuel blends, Fuel, 86(12-13), 2007, pp 1772-1780.
20. Indian standard code IS: 10000, 1980, Method of tests for internal combustion engines, Bureau of Indian Standards.
21. Indian standard code IS: 10003, 1981 Specification for performance requirements for compression ignition (diesel) engines for automotive purposes, Bureau of Indian Standards.
22. Indian standard code IS: 14273, 1999, Automotive vehicles- Exhaust emissions-gaseous pollutants from vehicles fitted with compression ignition engines-method of measurements, Bureau of Indian Standards.
23. Heywood, J.B., Internal Combustion Engine Fundamentals, International edition, McGraw-Hill Book Company, 1989.